arXiv:1707.08280v2 [astro-ph.GA] 19 Apr 2018

Radial Acceleration Relation by Dark Matter and Baryons in the Intermediate Acceleration Regime

Kyu-Hyun Chae,[1,2] Mariangela Bernardi,[2] and Ravi K. Sheth[2]

[1] *Department of Physics and Astronomy, Sejong University, 209 Neungdong-ro Gwangjin-Gu, Seoul 05006, Republic of Korea*

[2] *Department of Physics and Astronomy, University of Pennsylvania, 209 South 33rd Street, Philadelphia, PA 19104, USA*

(Dated: December 14, 2024)

We investigate the relation between radial accelerations due to the baryonic mass distribution ($a_{\rm B}$) and the dark (or phantom) matter distribution ($a_{\rm X}$) in the intermediate acceleration range $10^{-10} < a_{\rm B}/[{\rm m\ s^{-2}}] < 10^{-8.5}$. Our analysis is based on spherical Jeans modeling of nearly round pure-bulge (spheroidal, dispersion-supported) galaxies under ΛCDM and MOND paradigms. The galaxy sample contains 24 ATLAS$^{\rm 3D}$ galaxies with two-dimensional maps of stellar velocity dispersions and 4201 SDSS galaxies with fixed aperture mean stellar velocity dispersions. We find a correlation $a_{\rm X}/a_{\rm B} = 10^p (a_{\rm B}/C)^q$ with $p = -0.08 \pm 0.23$, $q = -0.85 \pm 0.20$ for $C = 1.2 \times 10^{-10}$ m s^{-2} and $a_{\rm B} > 10^{-9.5}$ m s^{-2}. Using a generalized MOND model of the form $a_{\rm B}/a = (a/a_0)/\left[1 + (a/a_0)^\nu\right]^{1/\nu}$ between the empirical acceleration a and the Newtonian prediction $a_{\rm B}$ by the baryons, we find $a_0 = (1.22 \pm 0.08) \times 10^{-10}$ m s^{-2} and $\nu = 0.88 \pm 0.15$ for $10^{-10} < a_{\rm B}/[{\rm m\ s^{-2}}] < 10^{-8.5}$. Our results constrain theories of dark matter or modified gravity.

Mass discrepancy in galaxies – the disagreement between the mass inferred from the observed light distribution and that derived from kinematics of stars and gases or gravitational lensing under the standard Newton-Einstein gravity and dynamics – remains an unsolved problem for fundamental physics and cosmology. Proposed resolutions of the mystery broadly fall into two classes: much of the gravitating mass is dark matter (DM), or our current understanding of gravity or dynamics must be modified (MG) [1].

Recent decades have witnessed the surprising observation that the mass discrepancy becomes prominent only when the (centripetal) radial acceleration is weaker than a characteristic value $a_0 \sim 10^{-10}$ m s^{-2}. In this regime, the observed radial acceleration traced by the circular velocity V, $a = V^2/r$, is well correlated with, but is not equal to the Newtonian radial acceleration predicted by the distribution of baryons, $a_{\rm B} = GM_{\rm B}(r)/r^2$, where G is Newton's gravitational constant and $M_{\rm B}(r)$ is the baryonic mass within a spherical radius r [2–4]. The radial acceleration relation (RAR, or mass discrepancy acceleration relation) is now well-established for rotating galaxies, particularly in the low acceleration regime $a_{\rm B} < 10^{-10}$ m s^{-2} [3, 4].

The empirical RAR $a = a(a_{\rm B})$ [or $a_{\rm B} = a_{\rm B}(a)$] can be written as

$$a(r) = G\frac{M_{\rm B}(r) + M_{\rm DM}(r)}{r^2} = \left(1 + \frac{a_{\rm DM}(r)}{a_{\rm B}(r)}\right) a_{\rm B}(r) \quad (1)$$

assuming DM halos, or

$$a(r) = f\left(\frac{a_{\rm B}(r)}{a_0}\right) a_{\rm B}(r) \text{ and } a_{\rm B}(r) = f^{-1}\left(\frac{a(r)}{a_0}\right) a(r) \quad (2)$$

assuming modified Newtonian dynamics (MOND) [5] or MG. In eq. (2) $f(x)$ is a fitting function, known as the interpolating function (IF), and $f^{-1}(y)$ its inverse function (or vice versa), respectively. These approaches can be parameterized in a unified way by introducing a 'phantom' matter in MG as follows:

$$\frac{a}{a_{\rm B}} - 1 = f\left(\frac{a_{\rm B}}{a_0}\right) - 1 \equiv \frac{a_{\rm X}}{a_{\rm B}}, \quad (3)$$

where X denotes dark or phantom matter.

Several functional forms (see Fig. 1) have been suggested to describe the existing data for rotating galaxies including the 'simple' function ($\nu = 1$, eq. 4) [6], the 'standard' function ($\nu = 2$, eq. 4) [7], and McGaugh's [8] function $f_{\rm McG}(x) = 1/\left(1 - e^{-\sqrt{x}}\right)$. We will consider the family of models indexed by ν,

$$f_\nu(x) = \left(\frac{1}{2} + \sqrt{\frac{1}{4} + \frac{1}{x^\nu}}\right)^{1/\nu} \text{ and } f_\nu^{-1}(y) = \frac{y}{(1 + y^\nu)^{1/\nu}}. \quad (4)$$

There exist a number of theoretical proposals of DM or MG that predict RARs. These range from Bekenstein's modified gravity [9], Verlinde's emergent gravity [10], a symmetron-like fifth force [11] and modified properties of DM such as superfluidity [12] or dipolarity [13]. The symmetron mechanism [11] predicts an RAR similar to McGaugh's or simple function. However, the rest of these theoretical proposals predict the same as, or similar to, the IF $f_{\rm Bek}(x) = 1 + 1/\sqrt{x}$. There also have been attempts to explain the empirical RAR within the standard Lambda cold dark matter (ΛCDM) paradigm using hydrodynamic-simulation [14–16] or semi-analytic approaches [17, 18]. However, ΛCDM can reproduce the empirical RAR only qualitatively [4, 15].

A recent series of studies [3, 4] argue that all galaxies follow the same RAR: McGaugh's function. However,

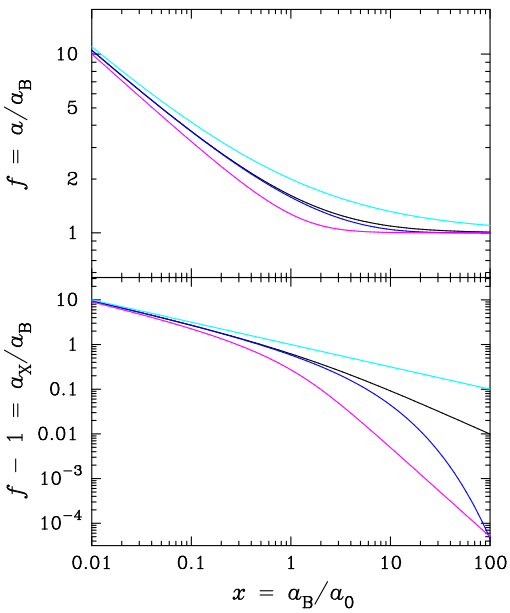

FIG. 1. Various fitting (interpolating) functions of the RAR in the form of $f = a/a_{\rm B}$ (top) or $f - 1 = a_{\rm X}/a_{\rm B}$ (bottom): (1) black: simple IF (eq. 4, $\nu = 1$), (2) magenta: standard IF (eq. 4, $\nu = 2$), (3) blue: McGaugh's IF, (4) cyan: Bekenstein's IF.

whether elliptical galaxies really do follow the same RAR as rotating disk galaxies is debated [19, 20]. Is there truly a Kepler-like law of RAR for all galaxies? If yes, what is the exact form of the RAR and what physics would be responsible for it? Would it be a manifestation of DM properties or gravity nature? With these questions in mind it is important to investigate the RAR of non-rotating elliptical galaxies.

From the viewpoint of the RAR, elliptical galaxies are distinct from rotating disk galaxies in two important ways. First, their stellar motions are dominated by random orbits, although they can have some net rotation, and/or possess rotating disks; in other words, they are dispersion(pressure)-supported systems as opposed to rotationally-supported. Secondly, their light profiles are more centrally concentrated, and thus the radial acceleration due to baryons is relatively high, typically $a_{\rm B} \gtrsim a_0$, in the optical regions within the effective radius $R_{\rm e}$, which is defined in galactic astronomy as the two-dimensional radius containing one half of the total light. On these scales, their dark or phantom matter is sub-dominant, leading to $a_{\rm X}/a_{\rm B} \lesssim 1$ within $R_{\rm e}$, as opposed to the typical situation $a_{\rm X}/a_{\rm B} \gtrsim 1$ with $a_{\rm B} \lesssim a_0$ in disk galaxies.

Moreover, Fig. 1 shows that the quantity $a_{\rm X}/a_{\rm B} = f - 1 = a/a_{\rm B} - 1$ can be distinguished between models when $a_{\rm B} \gtrsim a_0$. Crucially, the simple IF and McGaugh's IF are not well-separated in $a/a_{\rm B}$ but differ increasingly in $a_{\rm X}/a_{\rm B}$ as $a_{\rm B}$ gets larger. This difference in the high acceleration limit can have profound implications for the underlying physics [21]. Elliptical galaxies have the potential to constrain the functional form of the RAR for $a_{\rm B} \gtrsim a_0$ through the quantity $a_{\rm X}/a_{\rm B}$ (Fig. 1).

Here we investigate the RAR in the range $10^{-10} \lesssim a_{\rm B}/[{\rm m\ s^{-2}}] \lesssim 10^{-8}$ using Monte Carlo (MC) sets of models of nearly round pure-bulge (i.e. pure ellipsoids without detectable disks) galaxies, most of which have little net rotation, selected from the ATLAS$^{\rm 3D}$ sample [22] and the SDSS DR7 spectroscopic sample [23]. We have carried out spherical Jeans modeling and obtained MC sets of models for the selected galaxies under the ΛCDM and MOND paradigms. The galaxy data, modeling procedures and MC sets are described in detail in Ref. [24]. A concise description relevant to the RAR is given in the following.

We select 24 pure-bulges from the sample of 260 ATLAS$^{\rm 3D}$ galaxies as described in Ref. [24]. We also select pure-bulges from the UPENN spectroscopic catalog of ≈ 0.7 million galaxies [25]. We require SDSS galaxies to be statistically similar to the ATLAS$^{\rm 3D}$ pure-bulges [24]. The final sample of SDSS pure-bulges contains 4201 galaxies.

Under the spherical symmetry assumption all stellar motions in a galaxy are governed by the (radial) gravitational acceleration $a(r)$. Individual velocities and orbits of the stellar motions are not observed (or, hard to determine), but an rms scatter of the line-of-sight (LOS) velocity component, referred to as velocity dispersion (VD), is observed through Doppler broadening signatures of spectral lines. With the observed LOSVDs the spherical Jeans equation [26] – an equation required by the equilibrium state of elliptical galaxies – can be used to constrain $a(r)$. The acceleration is actually an combined effect, i.e. $a(r) = a_{\rm B}(r) + a_{\rm X}(r)$. On one hand, the Newtonian acceleration $a_{\rm B}(r)$ due to the distribution of baryons (meaning just stars for pure-bulges) $\rho_{\rm B}(r)$, could have been predicted by the observed light distribution $\rho_{\rm L}(r)$, if the stellar mass-to-light ratio $M_\star/L$ were known. To put it another way, the acceleration $a_{\rm B}(r)$ is actually an unknown depending on the unknown $M_\star/L$. On the other hand, the acceleration $a_{\rm X}(r)$ is also an unknown depending on the unknown dark or phantom distribution $\rho_{\rm X}(r)$. Therefore, the observed LOSVDs depend actually on the two unknowns, $M_\star/L$ and $\rho_{\rm X}(r)$. Our goal is to compare the accelerations $a_{\rm B}(r)$ with $a_{\rm X}(r)$. To this end $M_\star/L$ and $\rho_{\rm X}(r)$ have to be constrained simultaneously. However, there is one more unknown in connecting the observed LOSVDs with $a(r)$, namely the shape of the velocity ellipsoid at each point spanned by VDs in three directions. To account for anisotropic velocity ellipsoids we use the VD anisotropy parameter $\beta(r)$ defined by

$$\beta(r) = 1 - \sigma_{\rm t}^2(r)/\sigma_{\rm r}^2(r) \tag{5}$$

where $\sigma_{\rm r}^2(r)$ is the VD in the radial direction and $\sigma_{\rm t}^2(r) \equiv \left[\sigma_\theta^2(r) + \sigma_\phi^2(r)\right]/2$ is the mean VD in tangential (i.e. an-

gular in the spherical polar coordinates) directions.

For the ATLAS^{3D} galaxies 2-dimensional maps of LOSVDs are available within the central region up to $\sim R_e$ from which we construct a radial profile of LOSVDs, $\sigma_{los}(R)$ [24]. Throughout a capitalized R is used to refer to a radius on the projected plane. From the observed surface brightness distribution we also obtain a radial surface brightness profile $I(R)$ up to a few R_e's which in turn gives a volume density profile of luminosity $\rho_L(r)$ through deprojection.

Thus, for the ATLAS^{3D} galaxies we have two observed profiles, i.e. $\sigma_{los}(R)$ and $I(R)$, for three unknowns, i.e. the $M_\star/L$ profile $\Upsilon_\star(R)$, $\rho_X(r)$, and $\beta(r)$. In general, we have to face degeneracies among the unknown profiles in fitting the observed profiles. For this reason, it is necessary to use additional empirical constraints and/or make reasonable assumptions on the unknowns. In doing so, great care is required because specific assumptions may lead to biased results.

Our approach is to adopt well-motivated, flexibly parameterized models for the unknown profiles $\Upsilon_\star(R)$, $\rho_X(r)$ and $\beta(r)$. We then impose reliable empirical constraints on the models and allow the parameters of the models to be free within reasonable prior ranges. For $M_\star/L$ we adopt the model [24, 27]

$$\Upsilon_\star(R) = \Upsilon_{\star 0} \times \max\left\{1 + K\left[2.33 - 6(R/R_e)\right], 1\right\}, \quad (6)$$

which takes into account recent evidence of radial gradient in the central region ($< 0.4R_e$) [28–30] through 'gradient strength' parameter K: we consider a prior range $0 \leq K < 1.5$.

For DM density profile under the ΛCDM paradigm we adopt a generalized NFW (gNFW) [31] model given by

$$\rho_{gNFW}(r) \propto r^{-\alpha}\left[1 + c_{200}\left(\frac{r}{r_{200}}\right)\right]^{-3+\alpha}, \quad (7)$$

where inner slope α and concentration c_{200} are allowed to vary from the NFW values $\alpha_{NFW} = 1$ and c_{NFW}, and r_{200} refers to the radius of the sphere within which the DM density is 200 times the cosmic mean matter density. We use the prior range $0 < \alpha < 1.8$ for the inner slope and c_{200} is varied freely satisfying the constraint that the outer profile $r > 0.2r_{200}$ mimics the NFW. Under the MOND paradigm we use the generalized model given by eq. (4) with the prior range $0 < \nu \leq 2$.

For the VD anisotropy we use a generalized Osipkov-Merritt (gOM) model [26] given by

$$\beta_{gOM}(r) = \beta_0 + (\beta_\infty - \beta_0)\frac{(r/r_a)^2}{1 + (r/r_a)^2}, \quad (8)$$

where our prior range for the anisotropies is $-2 < \beta_{gOM}(r) < 0.7$ for all r and $0 < r_a < R_e$.

Now, the projected stellar mass density is $\Sigma_\star(R) = \Upsilon_\star(R)I(R)$ and the volume baryonic (i.e. stellar) mass density $\rho_B(r)$ is obtained by deprojection. With $\rho_B(r)$ and $\beta(r) = \beta_{gOM}(r)$ the spherical Jeans equation

$$\frac{d[\rho_B(r)\sigma_r^2(r)]}{dr} + 2\frac{\beta(r)}{r}[\rho_B(r)\sigma_r^2(r)] = -\rho_B(r)a(r) \quad (9)$$

allows one to predict the VD in the radial direction, $\sigma_r(r)$, for a given gravitational acceleration, $a(r)$, either eq. (1) (ΛCDM) or eq. (2) (MOND). The LOSVD at projected radius R on the sky is then given by [27]

$$\sigma_{los}^2(R) = \frac{1}{I(R)}\int_{R^2}^{\infty} \rho_L(r)\sigma_r^2(r)\left[1 - \frac{R^2}{r^2}\beta(r)\right]\frac{dr^2}{\sqrt{r^2 - R^2}}. \quad (10)$$

Finally, we obtain a MC set of models for each galaxy by first drawing $M_\star/L$ gradient strength K and DM halo parameters (or MOND IF parameters) from the above specified prior ranges and then finding $\Upsilon_{\star 0}$ and VD anisotropy parameters that best-reproduces the observed VDP: we do this by minimizing the goodness-of-fit static 'chi-squared'

$$\chi^2 = \sum_{i=1}^{N_{bin}} \frac{\left[\sigma_{los}^{obs}(R_i) - \sigma_{los}^{mod}(R_i)\right]^2}{s_i^2}, \quad (11)$$

where $\sigma_{los}^{obs}(R_i)$ is the measured LOSVD with its uncertainty s_i at R_i and $\sigma_{los}^{mod}(R_i)$ is the LOSVD predicted by the model under consideration. For most galaxies the global minimum of the reduced chi-squared $\bar{\chi}^2 \equiv \chi^2/N_{dof}$ (where the degree of freedom $N_{dof} = N_{bin} - N_{free} \approx N_{bin}$) is $\bar{\chi}^2_{min} \lesssim 2$ and we use only the models satisfying $\bar{\chi}^2 \lesssim 2\bar{\chi}^2_{min}$ for estimating the RAR for each galaxy.

Using the MC set of models we calculate the likely range of the acceleration ratio $a_X(r)/a_B(r)$ for the observed radial range of VDs for each galaxy. For each model the acceleration $a_B(r)$ is calculated using $\rho_B(r)$ deprojected from $\Sigma_\star(R) = \Upsilon_\star(R)I(R)$ for the constrained $\Upsilon_{\star 0}$ and K values. Under the ΛCDM paradigm $a_X(r) = a_{DM}(r)$ is calculated using the DM halo component while under the MOND $a_X(r)/a_B(r)$ is calculated using the model $a/a_B = f_\nu$ (eqs. 2 and 4) through $a_X/a_B = f_\nu - 1$ (eq. 3). Fig. 2 shows the distribution of $a_X(r)/a_B(r)$ for the models (satisfying $\bar{\chi}^2 \lesssim 2\bar{\chi}^2_{min}$) of each galaxy under the ΛCDM paradigm. Similar results are obtained under the MOND paradigm.

The ratio $a_X(r)/a_B(r)$ for an individual galaxy has a large scatter due to degeneracies among $M_\star/L$, DM distribution (or MOND IF) and VD anisotropy. Nevertheless, a trend appears when all median relations are put together as shown in Fig. 3. Although the statistical uncertainty (red dashed lines) is somewhat large, the simple case $\nu = 1$ in eq. (4) (black dashed curve) appears favored.

From the MC sets of models we estimate median values of $\langle K \rangle = 0.53^{+0.05}_{-0.04}$ and $\langle \beta_e \rangle = 0.05 \pm 0.25$ (radially averaged anisotropy within R_e). We also obtain the fundamental mass plane (FMP), a correlation of the effective radius R_e with the projected stellar mass $M_{\star e}$ and

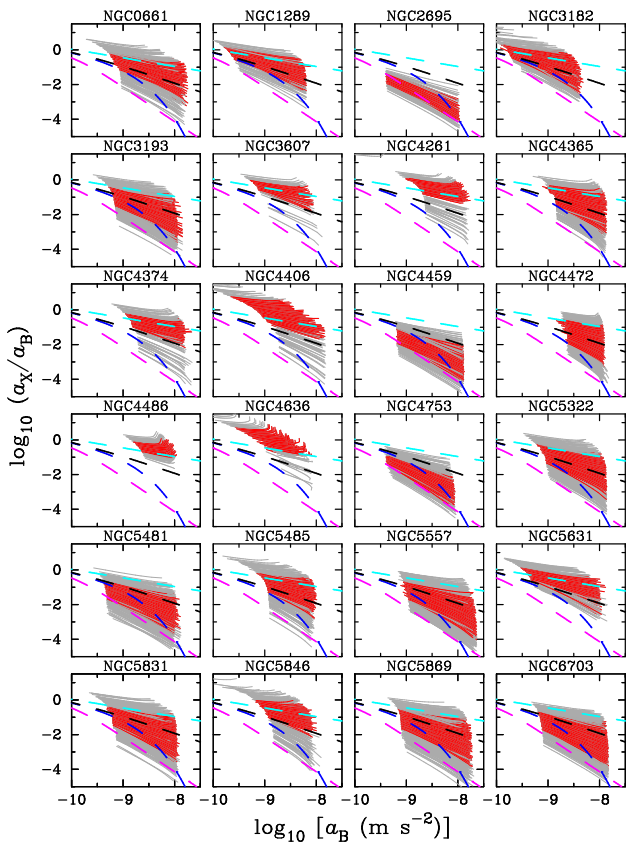

FIG. 2. Individual radial acceleration relation for 24 pure-bulge ATLAS^{3D} galaxies. Gray lines show predictions of all acceptable models in the sense $\bar{\chi}^2 < 2\bar{\chi}^2_{\rm min}$ and red lines represent 68 percent of the acceptable models. Here only the ΛCDM paradigm results are shown. Thick colored dashed curves represent various models/functions shown in Fig. 1.

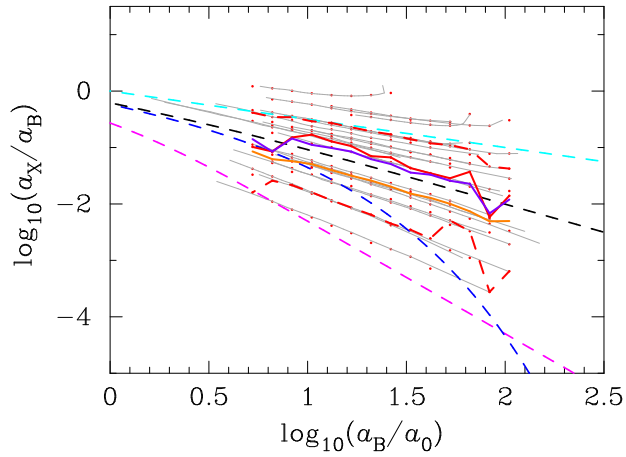

FIG. 3. Median radial acceleration relation for 24 pure-bulge ATLAS^{3D} galaxies whose individual results are displayed in Fig. 2. Thin gray lines represent individual medians. Red dots represent individual medians in uniform bins of $\log_{10}(a_B/a_0)$ with $a_0 = 1.2 \times 10^{-10}$ m s^{-2}. Thick red line connects the medians of the red dots in those uniform bins. Thick red dashed lines indicate 68 percent scatters. Orange line represents the results assuming no gradient ($K = 0$ in eq. 6) in $M_\star/L$. Purple line represents the results under the MOND paradigm. The background dashed curves represent various models/functions shown in Fig. 1.

the mean LOSVD $\sigma_{\rm e} \equiv \langle\sigma_{\rm los}(R)\rangle_{\rm e}$ within $R_{\rm e}$, in which $M_{\star{\rm e}} = M_{\star{\rm e}}(K)$ is a function of K: $\log_{10} M_{\star{\rm e}}(K) = \log_{10} M_{\star{\rm e}}(K=0) + b'K$ with $b' = -0.18^{+0.02}_{-0.07}$. We use these statistical results in modeling SDSS galaxies.

For the SDSS galaxy we have an averaged LOSVD within an aperture radius $R_{\rm ap} = D \times \theta_{\rm ap}$ in which $\theta_{\rm ap} = 1.5$ arcsec is the fixed angular aperture radius and D is the angular-size distance to the galaxy. Hence, we define the following light-weighted mean VD

$$\langle\sigma_{\rm los}\rangle(R) \equiv \frac{\int_0^R I(R')\sigma_{\rm los}(R')R'dR'}{\int_0^R I(R')R'dR'}, \qquad (12)$$

where $\sigma_{\rm los}(R)$ is given by eq. (10) and $I(R)$ is the surface brightness distribution. Then the aperture VD is given by $\sigma_{\rm ap} \equiv \langle\sigma_{\rm los}\rangle(R = R_{\rm ap})$.

The procedure of obtaining a MC set with the single dynamical constraint (i.e. $\sigma_{\rm ap}$) differs from that for an ATLAS^{3D} galaxy with a VDP for a radial range. Light distribution and DM halo (or MOND) parameters are drawn in the same way, but K is drawn from a range $0 \le K < K_{\rm max}$ where $K_{\rm max}$ is chosen so that the posterior distribution matches that for the ATLAS^{3D} galaxies. Then, $M_{\star{\rm e}}(K)$ is assigned using the FMP derived for the ATLAS^{3D} galaxies. Finally, we search iteratively for a VD anisotropy drawn randomly from a prior range (consistent with the ATLAS^{3D} galaxies) predicting $\sigma_{\rm ap}$ within the estimated error. If an anisotropy is not found within a pre-defined number of iterations $N^{(1)} = 20$, then we search for another predicting $\sigma_{\rm ap}$ within twice the error. If still not found within $N^{(2)} = 50$ iterations, then any anisotropy is taken from the prior range.

The MC sets of models for $\gtrsim 90$ percent of the SDSS galaxies satisfy the desired property that $\gtrsim 68$ percent of the models in a set predict $\sigma_{\rm ap}$ within the estimated error, as would be expected if all errors are approximately normal. We use those galaxies satisfying this property to calculate the ratio $a_{\rm X}/a_{\rm B}$ at $R_{\rm ap}$. The distribution of $a_{\rm X}/a_{\rm B}$ depends on the input values of $K_{\rm max}$ and b'. Also, the predicted distribution of VDP slopes depends on $K_{\rm max}$, b' and median anisotropy $\langle\beta_{\rm e}\rangle$. We require that the distribution of VDP slopes predicted by the combination $(K_{\rm max}, b')$ be consistent with what's observed in the ATLAS^{3D} galaxies for a choice of $\langle\beta_{\rm e}\rangle$ that is in the range derived for the ATLAS^{3D} galaxies. Our standard choice is $K_{\rm max} = 1$ and $b' = -0.18$.

The top panel of Fig. 4 shows the distribution of $a_{\rm X}/a_{\rm B}$ as a function of $a_{\rm B}$ for the standard choice under the ΛCDM paradigm. The bottom panel of Fig. 4 shows

the median (red-filled circles and thick gray curve) and the 68% scatters (gray dotted curves). We find a relation $a_{\rm X}/a_{\rm B} = 10^p(a_{\rm B}/C)^q$ with $p = -0.08 \pm 0.23$, $q = -0.85 \pm 0.27$ for $C = 1.2 \times 10^{-10}$ m s^{-2} and $a_{\rm B} \gtrsim 10^{-9.5}$ m s^{-2}. For the generalized MOND IF of eq. (4) we obtain $a_0 = (1.22 \pm 0.08) \times 10^{-10}$ m s^{-2} and $\nu = 0.88 \pm 0.15$. We can produce systematically shifted results by varying the input of $(K_{\rm max}, b')$. The bottom panel indicates two systematically shifted results for $K_{\rm max} = 0$ (lower curve) and $(K_{\rm max}, b') = (1, -0.25)$ (upper curve). These systematically shifted results (and any other plausible results) are within the estimated uncertainties.

Fig. 4 shows that only the simple IF (eq. 4, $\nu = 1$) is consistent with our modeling results of the SDSS galaxies as is the case for the ATLAS$^{\rm 3D}$ galaxies. The standard IF (eq. 4, $\nu = 2$), the theoretical IF and Verlinde's emergent gravity appear to be ruled out. McGaugh's fitting function is also inconsistent with our results at high accelerations $a_{\rm B} \gtrsim 10^{-9.5}$ m s^{-2}. In conclusion, our results characterized by $a_{\rm X}/a_{\rm B} \sim (a_{\rm B}/a_0)^q$ with $q \approx -1$ in the intermediate acceleration range point to a particular direction in theories of DM or MG.

We thank J. Khoury for interesting discussions about dark matter theories. We thank him and Mark Trodden for comments on the draft. We thank Michele Cappellari for useful communications regarding the ATLAS$^{\rm 3D}$ results. This work was carried out at the University of Pennsylvania while KHC was on sabbatical leave. This research was supported by Basic Science Research Program through the National Research Foundation of Korea (NRF) funded by the Ministry of Education (NRF-2016R1D1A1B03935804).

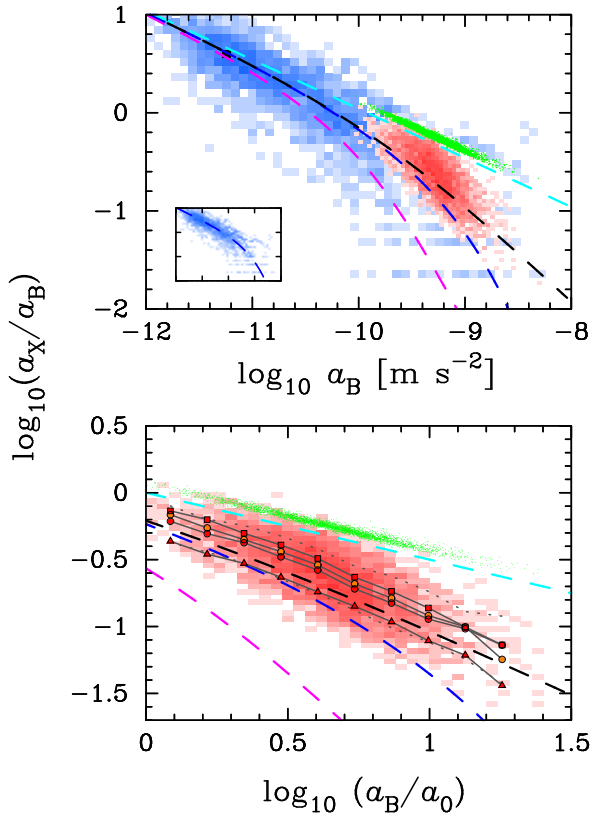

FIG. 4. Red pixels with varying intensity display the distribution of $a_{\rm X}/a_{\rm B}$ at $r = R_{\rm ap}$ as a function of $a_{\rm B}$ for 3991 galaxies for which modeling is successful with the standard input of $(K_{\rm max}, b') = (1, -0.18)$ under the ΛCDM paradigm as described in the text. Here $a_{\rm X} = a_{\rm DM}$ is the acceleration by the DM halo of each galaxy. Red filled circles represent the medians and the gray dotted curves show 68% scatters in the horizontal bins. Squares represent the systematically shifted result with $b' = -0.25$ while triangles represent the result with $K_{\rm max} = 0$. Orange circles shows the result with $(K_{\rm max}, b') = (1, -0.18)$ under the MOND model (eq. 4) where $a_{\rm X}/a_{\rm B} = f_\nu - 1$. Colored dashed curves are as in Fig. 1. Green points are predicted by Verlinde's emergent gravity. Blue pixels represent 2693 data points from rotating galaxies in the literature; these probe the low acceleration regime while our dispersion-supported galaxies probe higher accelerations. In the bottom panel $a_{\rm B}$ is normalized by $a_0 = 1.2 \times 10^{-10}$ m s^{-2}.

[1] B. Famaey, S. S. McGaugh, Living Rev. Rel. **15**, 10 (2012).
[2] S. S. McGaugh, Astrophys. J. **609**, 652 (2004).
[3] S. McGaugh, F. Lelli, and J. Schombert, Phys. Rev. Lett. **117**, 201101 (2016).
[4] F. Lelli, S. S. McGaugh, J.M. Schombert, and M. S. Pawlowski, Astrophys. J. **836**, 152 (2017).
[5] M. Milgrom, Astrophys. J. **270**, 371 (1983).
[6] B. Famaey, J. Binney, Mon. Not. R. Astron. Soc. **363**, 603 (2005).
[7] S. M. Kent, Astron. J. **93**, 816 (1987).
[8] S. McGaugh, Astrophys. J. **683**, 137 (2008).
[9] J. D. Bekenstein, Phys. Rev. D **70**, 083509 (2004).
[10] E. P. Verlinde, arXiv:1611.02269.
[11] C. Burrage, E. J. Copeland, P. Millington, Phys. Rev. D **95**, 064050 (2017).
[12] L. Berezhiani, J. Khoury, Phys. Rev. D **92**, 103510 (2015).
[13] L. Blanchet, A. Le Tiec, Phys. Rev. D **80**, 023524 (2009).
[14] A. D. Ludlow, A. Benitez-Llambay, M. Schaller, T. Theuns, C. S. Frenk, R. Bower, J. Schaye, R. A. Crain, J. F. Navarro, A. Fattahi, K. A. Oman, Phys. Rev. Lett. **118**, 1103 (2017).
[15] A. Tenneti, Y.-Y. Mao, R. A. C. Croft, T. Di Matteo, A. Kosowsky, F. Zago, A. R. Zentner, Mon. Not. R. Astron. Soc., **474**, 3125 (2018).
[16] B. W. Keller, J. W. Wadsley, Astrophys. J. Lett. **835**, 17 (2017).
[17] H. Desmond, Mon. Not. R. Astron. Soc. **464**, 4160 (2017).
[18] J. F. Navarro, A. Benítez-Llambay, A. Fattahi, C. S. Frenk, A. D. Ludlow, K. A. Omen, M. Schaller, T. The-

uns, Mon. Not. R. Astron. Soc. **471**, 1841 (2017).
[19] J. Janz, M. Cappellari, A. J. Romanowsky, L. Ciotti, A. Alabi, and D. A. Forbes, Mon. Not. R. Astron. Soc. **461**, 2367 (2016).
[20] O. Gerhard, A. Kronawitter, R. P. Saglia, R. Bender, Astron. J. **121**, 1936 (2001).
[21] B. Famaey, J. Khoury, R. Penco, J. Cosmol. Astropart. Phys., **03**, 038 (2018)
[22] M. Cappellari, et al., Mon. Not. R. Astron. Soc. **413**, 813 (2011).
[23] K. N. Abazajian, et al., Astrophys. J. Suppl. **182**, 543 (2009).
[24] K.-H. Chae, M. Bernardi, R. K. Sheth, Astrophys. J., submitted (arXiv:1804.00040)
[25] A. Meert, V. Vikram, M. Bernardi, Mon. Not. R. Astron. Soc. **446**, 3943 (2015).
[26] J. Binney, S. Tremaine, Galactic Dynamics, 2nd ed. (Princeton Univ. Press, Princeton, NJ, 2008).
[27] M. Bernardi, R. K. Sheth, H. Dominguez-Sanchez, J.-L. Fischer, K.-H. Chae, M. Huertas-Company, F. Shankar, MNRAS, in press (arXiv:1712.05414)
[28] P. van Dokkum, C. Conroy, A. Villaume, J. Brodie, A. J. Romanowsky, Astrophys. J. **841**, 68 (2017).
[29] I. Martín-Navarro, F. La Barbera, A. Vazdekis, J. Falcón-Barroso, I. Ferreras, Mon. Not. R. Astron. Soc. **447**, 1033 (2005).
[30] A. Sonnenfeld, A. Leauthaud, M. W. Auger, R. Gavazzi, T. Treu, S. More, Y. Komiyama, Mon. Not. R. Astron. Soc., submitted (arXiv:1801.01883)
[31] J. F. Navarro, C. S. Frenk, S. D. M. White, Astrophys. J. **490**, 493 (1997).